Spin dependent interface scattering, low temperature resistivity and magnetoresistance in NiFeCo/Cu superlattices

1998 J. Phys.: Condens. Matter 10 6659

(http://iopscience.iop.org/0953-8984/10/30/007)

J. Phys.: Condens. Matter **10** (1998) 6659–6676. Printed in the UK PII: S0953-8984(98)88259-3

Spin dependent interface scattering, low temperature resistivity and magnetoresistance in NiFeCo/Cu superlattices

Z T Diao†, S Tsunashima† and M Jimbo‡

† Department of Electronics, Nagoya University, Nagoya 464-01, Japan

‡ Material Engineering Laboratory, Daido Institute of Technology, Nagoya 457, Japan

Received 7 October 1997, in final form 21 April 1998

Abstract. The temperature dependence of the resistivity and magnetoresistance $\rho_{AF} - \rho_F$ of the NiFeCo (15 Å)/Cu (t_{Cu}) superlattices with $t_{Cu} = 9$ and 21–22 Å, characterized by different correlated interface roughness, is found to depend strongly on the nature of the dominant electron scattering centres in the interface zone, and is determined by that of the spin dependent interface resistivity. This explains why the magnetoresistance changes in a quite different manner with temperature from specimen to specimen. We propose, within the frame of a simplified two-current model, that the presence of spin fluctuations and/or spin glass states in the interface zone is responsible for the temperature dependent behaviour of the spin dependent interface resistivity. The main features of the derived interface resistivity data, such as a maximum at $T_{max} \simeq 12$ K for the specimen with $t_{Cu} = 9$ Å and a T^2, $T^{3/2}$ or T dependence for those with $t_{Cu} = 21$–22 Å, are explained satisfactorily in a unified picture of scattering of the electrons by spin fluctuations and/or spin glass states. The latter are in turn mediated appreciably by magnetic impurity concentration in the interface zone. The magnetoresistance at finite temperatures manifests itself to increase whenever the spin asymmetry is large, but to decrease with increasing magnetic impurity concentration in the interface zone.

1. Introduction

The temperature dependent behaviour of the electrical resistivity in magnetic superlattices, in which the Ruderman–Kittel–Kasuya–Yosida (RKKY)-type anti-ferromagnetic (AF) coupling and large magnetoresistance were observed, has been reported by several investigators [1–9]. Interest has been focused on the determination of the temperature dependence of the electronic transport properties and magnetoresistance, on the examination of intralayer bulk and interface scattering behaviour of the conduction electrons and on the comparison of the low temperature data with proposed theoretical models [10–12] that all took the two-current model of Fert and Campbell [13] as a prototype. In the earlier work of exploring the temperature dependence of the magnetoresistance in Fe/Cr superlattices either antiferromagnetically or ferromagnetically coupled, Mattson *et al* [4] showed that the resistivity and magnetoresistance at finite temperatures are primarily determined by the thermal excitation of magnons. They found at low temperatures T^2 and $T^{3/2}$ power laws in the magnetoresistance and T^2 and T^3 (phonon-assisted scattering) power laws in the s–d resistivity. The thermal excitations of magnons seem to decrease the magnetoresistance, but to increase the s–d resistivity, as the temperature increases. Later Duvail *et al* [14] demonstrated that a complete explanation of the temperature dependent magnetoresistance

0953-8984/98/306659+18$19.50

data for Co/Cu superlattices by considering the intrachannel bulk scattering and interchannel spin-mixing terms only is unobtainable unless incoherent scattering (with no scattering momentum conservation) by spin fluctuations at disorder interfaces is taken into account. More recently, to study the contribution from the interface zone to electron transport, Suzuki and Taga [9] constituted Co/Cu superlattices with artificial 'interface roughness' that was created by inserting at the interfaces very thin layers of atomic order in thickness. They argued that, upon increasing interface roughness, the residual resistivity changes significantly, but the residual magnetoresistance decreases; that the temperature dependence of the magnetoresistance is almost independent of interface roughness and that, rather than interface scattering, spin dependent intralayer bulk s–d scattering of the conduction electrons is crucial for the origin of the temperature dependent magnetoresistance.

At present, however, there are some points that still remain open to question and need to be addressed further. First, for example, in addition to the limitation of being valid only for ferromagnetic metals, the theoretical explanation [4] based on the concept of the thermal excitation of magnons totally ignores the existence of spin fluctuations at disorder interfaces. While such a theory can fit the temperature dependent resistivity and magnetoresistance data reasonably well, it would be completely inadequate to explain certain other complicated features of the contribution from rough interfaces to the electrical resistivity properties. This will be clear in what follows. Second, the nature of interfaces depends in a complicated manner on (1) roughness, including that with lateral coherence, and (2) interdiffusion at interfaces, or interplay of these different aspects. Though the inserting-layer-deposition engineering at interfaces [9, 15] has revealed that spin dependent interface scattering plays a significant role in determining magnetoresistance, the experimental approach of this type did not provide detailed information about how the nature of interfaces as mentioned above affects the resistivity and magnetoresistance. Thus, further studies that take as a beginning step a definite characterization of interface roughness are expected to yield more profound understanding of electronic transport properties in these superlattices.

This contribution is confined to the question of how low temperature electron transport in NiFeCo/Cu superlattices is influenced by the interplay of different aspects of interface roughness, in particular magnetic impurity interdiffusion across the interfaces. Considering intralayer spin dependent bulk scattering and interface scattering by magnetic impurities, we treat the low temperature resistivity data in the framework of the two-current model. We show the predominant importance of spin dependent interface scattering in determining the magnetoresistance observed, and relate it to the microscopic quantities of spin glass and/or localized-spin fluctuations. The main features of the temperature dependences of the interface resistivity as well as the magnetoresistance are found to change appreciably with magnetic impurity concentration in the interface zone, indicating the corresponding interplay between Kondo scattering and spin glass freezing. We demonstrate that interface roughness resulting from magnetic impurity interdiffusion at interfaces reduces greatly the spin asymmetry and then the magnetoresistance of these superlattice structures.

2. Experimental background

The specimens consist of four superlattices of a nominal form [NiFeCo (15 Å)/Cu (t_{Cu})]$_{20}$, buffered by 50 Å thick NiFeCo layers, one with $t_{Cu} = 9$ Å and the other three with $t_{Cu} = 21$–22 Å. All of them were prepared by means of the magnetron sputtering process and are polycrystalline with crystallographic (111) orientations in structure. Preparation details have been described elsewhere [16]. Polycrystalline superlattices may be produced which would necessarily have less well defined interfaces as compared with a single crystal

superlattice with atomically flat interfaces, but which could have fairly good registry as deposition rate stability and accuracy are guaranteed, for example, by precise, suitably corrected control of the power to magnetrons. In addition, interfaces rely for their well defined structure on being prepared on the buffer layer material properly chosen [17]. Structural characterization by means of x-ray diffraction and model fit to data [16, 17] has demonstrated that, for these superlattices, vertically correlated interface roughness is dominant which features the rms roughness, σ, and the lateral correlation length, ξ. We have shown that the magnetoresistance increases with increasing correlated interface roughness. Representative x-ray diffraction data for the superlattices with $t_{Cu} = 22$ Å, taken in the specular and rocking-curve geometry, are summarized in table 1.

Table 1. Values of vertically correlated interface roughness, σ_{corr}, lateral correlation length, ξ (after [16]), and the room temperature resistivities, ρ_F and ρ_{AF} in the ferromagnetic and AF states, magnetoresistance ($= (\rho_{AF} - \rho_F)/\rho_F$) and the corresponding extrapolated values at absolute zero, respectively, for the specimens of the form of [NiFeCo (15 Å)/Cu (t_{Cu})]$_{20}$ grown on 50 Å thick NiFeCo buffer layers.

			Resistivity					
			$T = 0$ K		$T = 300$ K		Magnetoresistance	
Specimens	Roughness σ_{corr} (Å)	Correlation length ξ (Å)	ρ_{AF} ($\mu\Omega$ cm)	ρ_F ($\mu\Omega$ cm)	ρ_{AF} ($\mu\Omega$ cm)	ρ_F ($\mu\Omega$ cm)	$T = 0$ K	$T = 300$ K
							(%)	
$t_{Cu} = 9$ Å								
A	—	—	41.48	26.34	50.00	39.36	57.5	27.0
$t_{Cu} = 21$–22 Å								
B	5.64	240	18.79	15.30	23.44	21.00	22.9	11.6
C	5.49	180	21.14	17.91	26.70	24.60	18.00	8.5
D	4.24	307	16.76	14.3	21.77	20.60	17.0	5.7

Resistance and magnetoresistance measurements, in which a magnetic field of 5 kOe was applied parallel to the current, were made at the temperatures ranging from 5 to 300 K using a standard four-point probe technique. The operating current, provided by a GPIB controlled constant current source, was 0.1 mA. It was reversed many times during measurements at each temperature so as to avoid the influences of the complicated thermoelectric effects. Each measured point represent an average of the results obtained on at least ten experimental runs. The temperature was stabilized and measured to better than 0.5%. Area to length ratios for the specimens were determined to within 0.5% thus allowing reliable estimates of impurity resistivity to be made. The corresponding magnetization curves were measured utilizing a vibrating sample magnetometer, in which both the current and the magnetic field were applied parallel to the hard in-plane axis of the film.

3. Results and data analysis

The magnetoresistance and magnetization versus field curves measured at room temperature are shown in figure 1 for two specimens of the form [NiFeCo (15 Å)/Cu (t_{Cu})]$_{20}$, with $t_{Cu} = 9$ and 22 Å, corresponding to the first and second AF coupling peaks, respectively. The specimen A at $t_{Cu} = 9$ Å shows the characteristic shearing and low remanent moment at zero field; whereas the specimen B at 22 Å exhibits increasing ferromagnetic character, showing a comparatively large remanent moment, with a value of M_r/M_S estimated to be $<10\%$, because of the occurrence of intermixed regions. The magnetic coupling

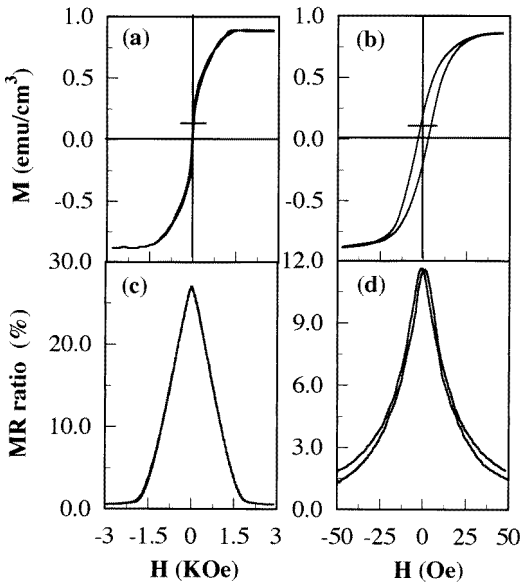

Figure 1. Magnetization and resistivity versus field curves, measured in the in-plane hard direction at room temperature, for the specimens of a nominal structure of the form [NiFeCo (15 Å)/Cu (t_{Cu})]$_{20}$ grown on a 50 Å thick NiFeCo buffer layer, with $t_{Cu} = 9$ Å (A) in (a) and (c), and $t_{Cu} = 22$ Å (B) in (b) and (d).

strength decays rapidly with an increase in spacer layer thickness due to the damped long-range oscillatory behaviour of the RKKY interaction. This is reflected by a significant difference of almost two orders of magnitude in saturation fields. On the other hand, the magnetoresistance decays much more slowly as approximately the inverse Cu layer thickness. At $t_{Cu} = 22$ Å, magnetoresistance values of less than half that at $t_{Cu} = 9$ Å are found for saturation fields more than 50 times smaller. Care should be paid here when one deals with the magnetic and electronic transport properties of these superlattices. The reason for this is that, for the specimens at $t_{Cu} = 22$ Å, it is unreliable to determine the degree of AF coupling only by taking a glance at the change of the remanant magnetization and then relate this to the resistance data. Evidence can be found in our previous work [18], where for large values of the ratio of $(1 - M_r)/M_S$ the magnetoresistance in fact becomes insensitive to the size of this parameter.

For the two representative specimens, the variations of the resistivity with temperature in both the ferromagnetic and AF states are shown in figure 2; and the corresponding variations of the magnetoresistance ($= \rho_{AF} - \rho_F$) with temperature in figure 3. Note that we defined the magnetic states at $H = 0$ as the AF states, and that is thought to be reasonable since the coercive field, H_c, is negligibly small compared to that of Co/Cu superlattices. This is true because we adopted a selected composition of $Fe_{16}Ni_{66}Co_{18}$ for the magnetic layer material, featuring both zero magnetocrystalline anisotropy and zero magnetostriction constants, so as to give excellent soft magnetic performances. Therefore, little error in the evaluation of our data between different definitions of magnetoresistance at $H = 0$ and $H = H_c$ is allowed in this experiment. What is more, the temperature variation of the coercive field is very small then so should its influence be on the change in the magnetization process with temperature. This means that the shape of the magnetoresistance variation versus temperature is influenced

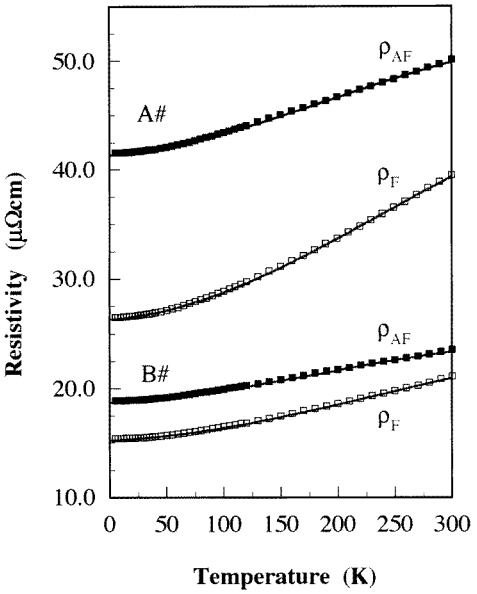

Figure 2. Resistivity as a function of temperature for the specimens appearing in figure 1 in both the ferromagnetic and AF states. The solid lines are a guide to the eye.

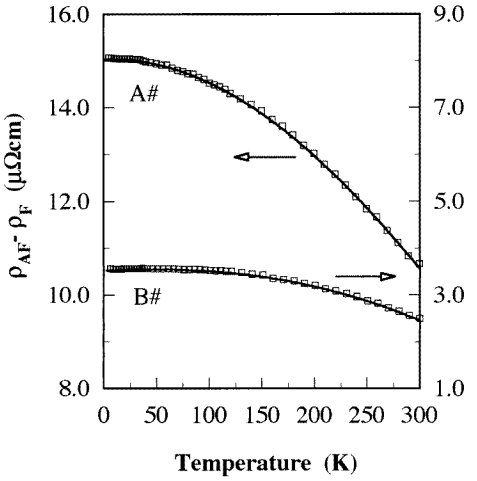

Figure 3. Magnetoresistance, $\rho_{AF}-\rho_F$, as a function of temperature for the specimens appearing in figure 1. The solid lines are a guide to the eye.

little by the change in the magnetization process with temperature.

The magnetoresistance as shown in figure 3 tends to increase linearly with decreasing temperature at higher temperatures and then to saturate at low temperatures. The specimen A at $t_{Cu} = 9$ Å shows a large temperature variation in the resistivity and magnetoresistance over the whole temperature range (figures 2 and 3); and its magnetoresistance amounts to almost three times that for the one with $t_{Cu} = 22$ Å. The difference can be thought of as due to the interplay of the mean free path effect and the inelastic scattering processes mediated

by magnons. The effects become increasingly important in determining the behaviour of the temperature dependence of the resistivity and magnetoresistance at the nitrogen temperature or higher. It has been shown that the magnetoresistance will vanish as $\exp(-t_{Cu}/\lambda_{MFP})$, where λ_{MFP} is a length of the order of the mean free path and is temperature dependent [1, 19]. The reduction of λ with increasing temperature enhances t_{Cu}/λ_{MFP} and then reduces the magnetoresistance. However, the mean free path effect alone is insufficient to account completely for such a large difference in the magnetoresistance data unless the strikingly different spin asymmetry factor α for the two specimens (table 2) and the magnon induced inelastic scattering process that would be of equal importance are invoked in discussions (also see [2]).

Table 2. Parameters characterizing the spin dependent resistivity, interface resistivity and spin asymmetry at low temperatures for the specimens of the form of [NiFeCo (15 Å)/Cu (t_{Cu})]$_{20}$ grown on 50 Å thick NiFeCo buffer layers.

Specimens	$\alpha(=\rho_{0\downarrow}/\rho_{0\uparrow})$	$\mu(=\rho_{i\downarrow}/\rho_{i\uparrow})$	$\rho_{0I\uparrow}(\mu\Omega$ cm)	$\rho_{0I\downarrow}(\mu\Omega$ cm)
$t_{Cu} = 9$ Å				
A	4.05	1.58	72.28	337.30
$t_{Cu} = 21$–22 Å				
B	2.52	1.58	51.40	133.50
C	2.28	1.38	67.06	152.83
D	2.23	1.32	64.95	143.48

The temperature dependences of the magnetoresistance for the specimens B, C and D are exhibited in figure 4, and the relevant physical quantities are summarized in table 1. Obviously the magnetoresistance curves away from linearity that is predominant at high temperatures, or bends towards the slowly varying region for specimen C (b) at moderate temperatures. At low temperatures, for the specimens B (a) and C (b), it tends to saturate as the temperature decreases; but for the specimen D (c), the magnetoresistance rises steeply, initially quite slowly at the nitrogen temperature region, and then approximately linearly with temperature again. The features of the variations of the magnetoresistance with temperature here are similar to those as shown in figure 3, but the difference in them reflects the influence of rough interfaces upon the magnetoresistance as a function of temperature. As has been apparent in our previous study [16], at room temperature, a large magnetoresistance is associated with rougher interfaces that are described in terms of correlated interface roughness. This is also the case in the present situation in which the variation of the magnetoresistance with temperature is under consideration. Besides, we notice that the difference is most striking at low temperatures. In figure 5, the temperature dependent parts of the magnetoresistance at the low temperature region (< 40 K) are plotted in detail for all these superlattices, showing behaviour much more complicated than that observed in Fe/Cr superlattices [4]. The magnetoresistance is found to decrease with increasing temperature for all the specimens, except for the specimen B; in addition, a marked 'knee' variation in decreasing magnetoresistance with temperature is seen for the specimen A, and that has not been reported in the existing literature. It is known that many sources, such as extrinsic structural factors and exchange coupling, may be responsible partially for the temperature dependence of the resistivity and magnetoresistance in superlattices. First, using buffer layers, with the resistivity smaller than that of the stacking of multilayer structure itself, may cause the shunting effects of the current in superlattices [20]. What is more, the bilayer number of superlattices, reflecting the strength of scattering of the conduction

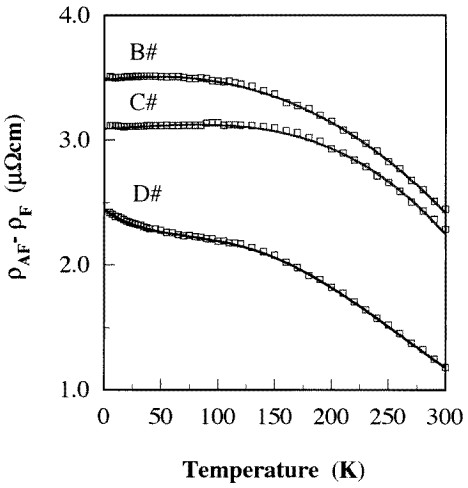

Figure 4. Magnetoresistance, $\rho_{AF} - \rho_F$, as a function of temperature for the specimens B, C and D, with $t_{Cu} = 21$–22 Å. The structural features of all these specimens are delineated by correlated interfacial roughness (table 1). The solid lines are a guide to the eye.

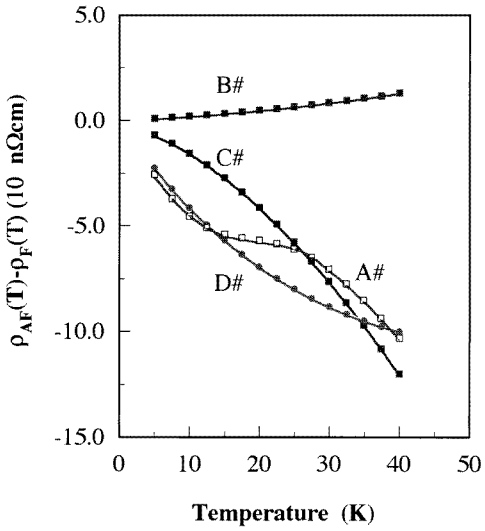

Figure 5. Temperature dependent part of the magnetoresistance, $\rho_{AF} - \rho_F$, at low temperatures for the specimens A, B, C and D, showing the distinctly different behaviour of their temperature dependences.

electrons at interfaces, alters the values of the magnetoresistance [11]. All these structural factors influence significantly the magnetoresistance and its temperature dependence, and allow an additional visualization of variation as the temperature varies. However, such a kind of variation of the magnetoresistance with temperature can be completely neglected in this experiment since we utilized the same material as that of the magnetic layers and made the bilayer number of all the specimens fixed. Second, the temperature dependence of exchange coupling which derives from the temperature disordering of the magnetic

moments, especially those at interfaces, is an artifact of obtaining exchange coupling from magnetization measurements. Since the magnetization, at least in the temperature range of interest, does not vary so much with temperature, the variation of the degree of AF alignment with temperature is out of the question in the present case. It has been also shown in the previous theoretical work [21] that at low temperatures the strength of interlayer coupling is almost independent of temperature for superlattices with thicker magnetic layers.

To obtain some idea of what happens to the electronic transport properties in our superlattice structures, the distinguishable resistivity and magnetoresistance data are analysed in the frame of the two-current model; and the derived contribution of the interface zone is tentatively explained by relating it to the Kondo effects and spin glass phenomena. Essentially, the conventional approach of the two-current model assumes that the spin up and down conduction channels contain nearly free electrons that carry the current in parallel. In the low temperature range, in which the residual resistivities, $\rho_{0\uparrow}$ and $\rho_{0\downarrow}$, are much larger than the temperature dependent resistivities, $\rho_{i\uparrow}(T)$, $\rho_{i\downarrow}(T)$ and $\rho_{\uparrow\downarrow}(T)$, this model predicts the temperature dependent resistivity as [13]

$$\rho_F(T) - \rho_{F0} = \left(1 + \frac{(\alpha-\mu)^2}{(1+\alpha)^2\mu}\right)\rho_i(T) + \frac{(\alpha-1)^2}{(\alpha+1)^2}\rho_{\uparrow\downarrow}(T) \tag{1}$$

where

$$\rho_{F0} = \frac{\rho_{0\uparrow}\rho_{0\downarrow}}{\rho_{0\uparrow}+\rho_{0\downarrow}}$$

$$\rho_i(T) = \frac{\rho_{i\uparrow}(T)\rho_{i\downarrow}(T)}{\rho_{i\uparrow}(T)+\rho_{i\downarrow}(T)}$$

and

$$\alpha = \rho_{0\downarrow}/\rho_{0\uparrow} \qquad \mu = \rho_{i\downarrow}(T)/\rho_{i\uparrow}(T).$$

Here, in general, both phonon and magnon assisted scatterings contribute to the temperature dependent resistivity $\rho_{i\sigma}(T)$, but only the magnon assisted scattering contributes to the spin mixing resistivity $\rho_{\uparrow\downarrow}(T)$. (1) can be directly applied to the present superlattice structures in the ferromagnetic states. Once the superlattice structures lie in the AF states, the resistivities of the two channels are the same, and, therefore, the corresponding total resistivity can be written as

$$\rho_{AF} - \rho_{AF0} = \frac{\rho_{i\uparrow}(T) + \rho_{i\downarrow}(T)}{4} \tag{2}$$

which holds at any temperatures and is, in fact, simply an analogue of the high temperature limit of the resistivity for bulk materials. In this circumstance, the spins are completely mixed so that the resistivity for each spin channel will be given by averaging both the spin up and down resistivities.

In the case of superlattice structures (1) and (2) hold with the requirement that the additive law of the resistivity apply in each conduction channel, that is,

$$\rho_{i\sigma} \approx \frac{2\rho_N t_N + \rho_{M\sigma} t_M + 2\rho_{I\sigma} t_I}{t_N + t_M + 2t_I} \tag{3}$$

where ρ_N, $\rho_{M\sigma}$ and $\rho_{I\sigma}$ ($\sigma = \uparrow$ and $\downarrow$) are, respectively, the resistivities of the nonmagnetic spacer layer, magnetic layer and interface zone, with the corresponding thicknesses of t_N, t_M and t_I. The statement is true for the present superlattices and the reason for this is as follows. In experimental view of the magnitude of the resistivity in table 1, the effective mean free path (elastic scattering length) is evaluated to be 120 Å for the specimen A and 220 Å for the specimens B, C and D, with reference to the relation of $\rho l = 31.5 \times 10^{-6}$ $\mu\Omega$ cm^2

obtained for single crystal Permalloy films [22], respectively. They all are larger than the characteristic length scale of individual layer thickness. Of course, this would not be the whole story for the spin dependent mean free paths of the magnetic materials. We roughly estimated α ($\approx l_\uparrow/l_\downarrow$) ≈ 2 from our resistance data for single NiFeCo films and noted that this value is in fact a greatly reduced one compared to those given by Dieny *et al* [23]. This suggests a longer mean free path for either spin up or spin down electrons in the present magnetic films and superlattice structures. The findings here are that the mean free path for spin up electrons is constantly larger than the thickness of the layer; and that of spin down electrons is smaller than 80 Å. We take this to mean that in a certain condition our assumption made above can be considered to reasonably approximate on average the experimental entities. Since the averaging of the relaxation times in the two different layers allows an additive law for the integrated resistivity [24, 25], we are able to make use of the additive law to give a thickness–weight-averaged total resistivity for each spin channel considering interface zones as separate phases where the size is characterized by correlated interface roughness.

While treating the resistivity and magnetoresistance data, we would relate the derived interface resistivity to scattering of the conduction electrons by spin glass states and spin fluctuations. Several important aspects of the magnetic resistivity of this type have to be accounted for in advance. As known, for a spin glass system containing magnetic impurities located at random, without well defined long range order at any temperature, the magnetic resistivity due to scattering of conduction electrons by the elementary excitation of the system is given by [26].

$$\rho_{RA}(c, T) = \rho_{RA}(c) + A(c)T^{3/2} \tag{4}$$

in which c represents magnetic impurity concentration, and $\rho_{RA}(c)$ and $A(c)$ are the constant coefficients. The residual resistivity $\rho_{RA}(c)$ is due to resonant scattering from a spin split virtual bound state; and $A(c)$ depends on the magnetic state of the impurity spins and the RKKY type coupling constant. In this physical picture, any spin-flip excitations on an impurity site are unable to propagate like a magnon, but die away with some diffusion constant. At low temperatures, the conduction electrons are scattered by independent localized spin fluctuations of lifetime $\tau_{sf} = (\Lambda q^2)^{-1}$, where q labels the modes available and Λ is a diffusion constant. The behaviour of the resistivity depends critically on the availability of diffusion modes with damping rate Λq^2 approaching zero. At the other extreme, when each spin is damped independently, each mode contributes to the resistivity like an ordinary localized spin fluctuations (LSFs) of lifetime $(\Lambda q^2)^{-1}$, i.e., $(k_B T/\Lambda q^2)^2$ at low temperatures. Consequently the resistivity will go like T^2 instead of $T^{3/2}$ for temperatures $k_B T < \Lambda q_0^2$.

In the limit when the impurities are much less concentrated and the RKKY interaction between them is far larger than the Kondo fluctuation temperature, T_K, the locking in of the impurity spins below the freezing temperature, T_f, destroys the development of the delicately balanced LSF resonant state and reduced the spin-flip scattering between impurity and conduction electron spins. Theoretically, it is possible to account for the magnetic resistivity by assuming that the impurity spins consist of interacting spins and, at least above T_f, effective free spins that obey the Curie–Weiss law of susceptibility. These spins would experience different local fields; and statistically their population levels obey the Boltzmann distribution in the classic limit. Accordingly, the magnetic resistivity owing to scattering of the conduction electrons by the twofold scattering centres is given by [27]

$$\Delta\rho(c, T) = \Delta\rho_{RA}(c, T)(1 - \exp(-E_C/k_B T)) + \Delta\rho_K(c, T)\exp(-E_C/k_B T) \tag{5}$$

and

$$\rho_K(c,T) = \rho_K(c) - D(c)\ln(T^2 + (E_C/k_B)^2)^{1/2} \tag{6}$$

where $\rho_K(c)$ and $D(c)$ are constant coefficients, and $E_C = g\mu_B H_C$ [28]. $\Delta\rho(c,T)$ in (5) represents the temperature dependent part of the modified Kondo or spin fluctuation resistivity for single impurity spins of concentration c, in which the temperature is replaced by $T_{eff} = (T^2+(E_C/k_B)^2)^{1/2}$, with $T_m = E_C/k_B$ [29]. The logarithmic nature of the Kondo effect means a limit of localized spin fluctuation with a long lifetime τ_{sf} as a reasonable approximation for effective free spin; and the spin fluctuation resistivity will be suppressed by the local internal fields as the temperature decreases.

Note here that the Kondo effects and spin glass phenomena were originally found in magnetically dilute bulk alloying systems, for example, the isolated magnetic impurity Fe or Mn dissolved in an otherwise nonmagnetic host metal Cu, Ag or Au. Here acquiring a moment for a magnetic impurity and small Kondo temperature are prerequisite conditions for the observation of these effects. For the present superlattice structures, however, the situation is quite different: impurity atoms dissolved at the nonmagnetic spacer layer side distribute in the proximity of magnetic layers and are subject to the significant influence of adjacent magnetic layers. The presence of localized magnetic moments on impurity atoms, albeit originally impossible in the case of bulk alloying systems, might come close to reality in the superlattice structures. Evidence can be found in CoNi/Cu superlattice systems, where the localized magnetic moments are evaluated to be, respectively, 1.6 and 0.45 μ_B/atom for Co and Ni impurities in Cu [30]. On the other hand, in the concentrated nearly magnetic regime featured by the environment of groups of impurity distribution, a large reduction of T_{sf} $(= \hbar/k_B\tau_{sf})$ due to the local spin enhancement has been observed, as is the case in Cu–Ni, Cu–Co, Cu–Fe and Cu–(Ni,Fe) alloying systems [31–36]. Thus, for the superlattice structures with magnetic NiFeCo alloying layers, there is the large possibility for Fe, Co and Ni impurities appearing at the Cu spacer layer side that contribute magnetically to the possible Kondo effects and spin glass phenomena.

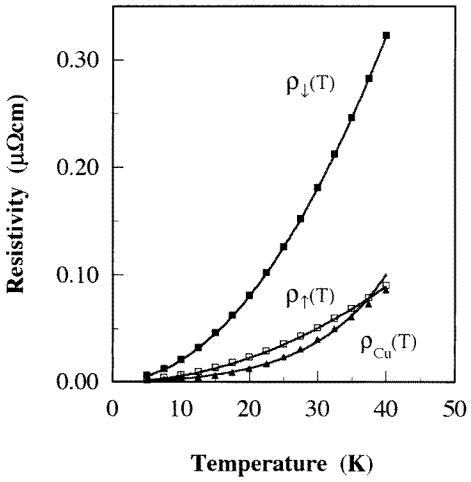

Figure 6. Temperature dependent part of the resistivity of a single Cu film, and of the spin dependent resistivity of a representative as-deposited NiFeCo film.

Figure 6 shows, along with the experimental resistivity data for a single Cu film, the calculated results of the temperature dependent part of the spin dependent resistivity,

$\rho_\uparrow(T)$ and $\rho_\downarrow(T)$, for a representative single NiFeCo film of ~1200 Å thick. All these results constitute a database for the detailed analysis of the low temperature resistivity and magnetoresistance in the superlattice structures. $\rho_\uparrow(T)$ and $\rho_\downarrow(T)$ are calculated using (1), provided that the relevant results of the spin mixing term $\rho_{\uparrow\downarrow}(T)$ for Ni metals in [13] apply in this case, and $\mu(=\rho_{i\downarrow}(T)/\rho_{i\uparrow}(T))$ can be approximately taken as a constant. The second assumption is reasonable though μ is in general weakly temperature dependent in the low temperature range of interest. While dealing with the resistivity data for magnetic films, care should be taken since the magnetic induction $B(=H+4\pi M_S)$ is also acting on the conduction electrons in ferromagnetic metals. The experimental resistivity data taken at $H=0$ may include a term due to the normal magnetoresistance effect of the spontaneous magnetization $4\pi M_S$ [37]. For the purpose of practicing a comparison between experiment and theory, the data given at $B=0$ should be used. All the experimental data used here were obtained from the resistance measurements on as-deposited NiFeCo film specimens in the condition of $B=0$.

The temperature dependent parts of the low temperature resistivity in the ferromagnetic and AF states, $\rho_F(T)$ and $\rho_{AF}(T)$, for the specimen A are plotted in figure 7(a). The curvature towards a higher power in temperature, stronger than linear, is observed in the resistivities. The difference in the curvature in the two magnetic states leads to a marked 'knee' variation of the magnetoresistance with temperature (figure 5), and serves as an indicator of the complicated intrachannel interface scattering in origin. The corresponding temperature parts of the spin dependent interface resistivities, $\rho_{I\sigma}(T)$ ($\sigma=\uparrow$ and $\downarrow$), are shown in figure 7(b). They are derived utilizing (1) and (2) from the difference of the resistivities in the two different magnetic states. Following the work of Duvail *et al* [14],

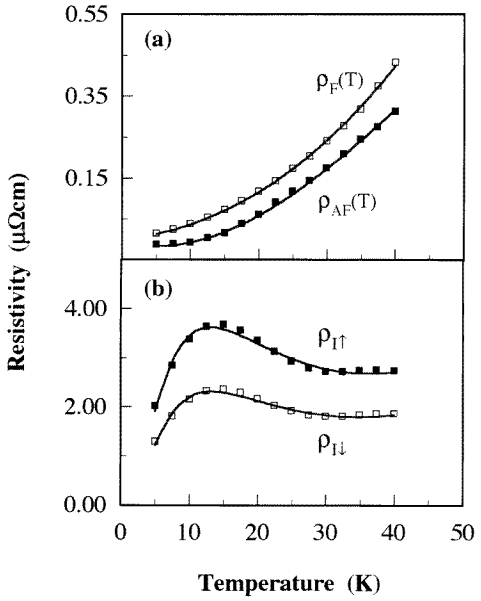

Figure 7. Temperature dependent part of the resistivity in both the ferromagnetic and AF states (a), and of the spin dependent interface resistivity (b) for the specimen A. The solid lines in (a) are a guide to the eye; while those in (b) show the results of a model fit to the resistivity data. The resistivity maximum at $T \simeq 12$ K is attributed to the combined effect of localized spin fluctuations and spin glass phenomena.

the spin mixed scattering at interfaces in this model fit was neglected. The resistivity due to intralayer bulk scattering was described by the data as shown in figure 6, and the spin mixing term $\rho_{\uparrow\downarrow}(T)$ was treated in a similar way as mentioned above. To model-fit $\rho_{I\sigma}(T)$ for the specimen A, a lower limit of correlated interface roughness was assumed to be of 4 Å with reference to the relevant structural data for other. As seen from figure 7(b), upon increasing the temperature, both of $\rho_{I\sigma}(T)$ rise initially faster than T, and then roughly linearly as the temperature further increases. At higher temperatures, they increase slower than T and show a well defined resistance maximum before decreasing again. This behaviour was satisfactorily fitted by applying (5). The coefficients for model fit are, with $T_m = 30.64$ K, $A(c) = 0.11(0.18)$ $\mu\Omega$ cm K$^{-3/2}$ and $D(c) = 7.48(11.82)$ $\mu\Omega$ cm ln^{-1} K for the spin up (down) channels.

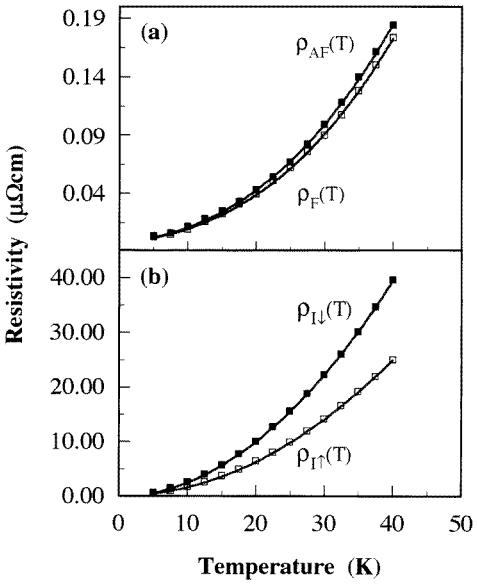

Figure 8. As for figure 7 but for the specimen B. The solid lines in (b) show the T^2 dependence of the interface resistivity due to the magnetic-impurity-assisted scattering process.

In a similar manner, figures 8–10 show, respectively, the temperature dependent parts of the low temperature resistivities $\rho_F(T)$, $\rho_{AF}(T)$ and $\rho_{I\sigma}(T)$ for other three specimens B, C and D. It can be seen that both $\rho_F(T)$ and $\rho_{AF}(T)$ for all the three specimens exhibit, as a whole, a much weakened temperature dependence as compared to that for the specimen A. This can be explained in terms of the mean free path effect as mentioned above. Another remarkable feature is that there is an increasing difference between $\rho_F(T)$ and $\rho_{AF}(T)$ over the whole temperature range of interest from the specimen B to D. We believe that it indicates the importance of spin-glass-like scattering of the conduction electrons by magnetic impurities at rough interfaces that will be discussed in section 4. Moreover, for both of the specimens C and D, $\rho_F(T)$ varies much more rapidly with temperature than does $\rho_{AF}(T)$. The latter one is marked by a resistivity minimum that is observed to locate in the temperature range of 15–20 K shifting toward the higher temperature side as the specimen changes from C to D. Notice here that the resistivity minimum in $\rho_{AF}(T)$ does not appear in $\rho_{I\uparrow}(T)$ or $\rho_{I\downarrow}(T)$ in figures 9 and 10. The reason for this difference is as follows. First, mathematically spin dependent resistivities with clear physical meaning

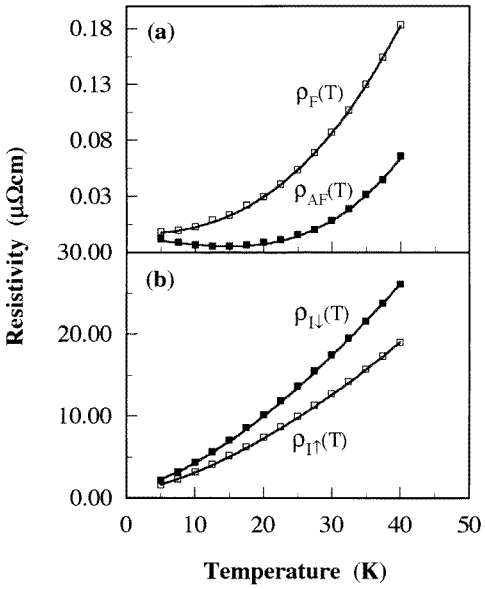

Figure 9. As for figure 7 but for the specimen C. The solid lines in (b) show the $T^{3/2}$ dependence of the interface resistivity due to the magnetic-impurity-assisted scattering process.

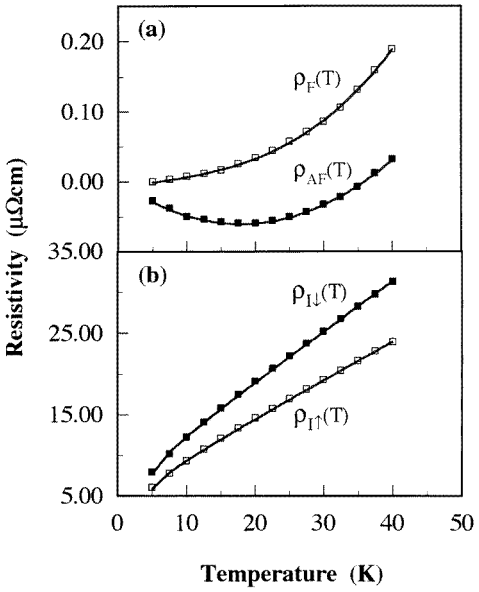

Figure 10. As for figure 7 but for the specimen D. The solid lines in (b) show the T dependence of the interface resistivity down to 10 K, due to the magnetic-impurity-assisted scattering process.

in the frame of the two-current model can be determined only by solving (1) and (2) together, i.e., by calculating the magnetoresistance $\rho_{AF} - \rho_F$. Thus, the behaviour of the spin dependent interface resistivities are not necessarily the same as what we observed in the AF states. Second, what is more important, unlike simple Kondo alloys there is physically

no guarantee that the resistivity minimum is always related to the Kondo effect, though it is often reminiscent of the existence of the effect in magnetic superlattice structures. Evidence for the statement can be found in previous work by Saito *et al* on Co/Cu superlattices [6] in which the resistivity minimum observed at about 10 K was explained by the T dependence of the magnetoresistance and saturation resistivity (of course, on the other hand, we were also aware of the example of showing the effect in Au/Fe superlattices given by Sato *et al* [5]). At present the absence of the effect in these specimens can be further understood in a somewhat different way by examining the experimental data for $\rho_F(T)$. No resistivity minimum being observed in $\rho_F(T)$ constitutes elegant evidence for the present argument because magnetic field depreciation cannot eliminate the Kondo effect completely if the effect does really exist, as shown by the experimental data for AuCuFe systems [38].

The spin dependent interface resistivities $\rho_{I\sigma}(T)$ for the specimen B are illustrated in figure 8, obeying a T^2 power law with coefficients of 15.5 (24.6) nΩ cm K^{-2} for the spin up (down) channels. Those for the specimen C follow a $T^{3/2}$ power law (figure 9) and are best described by (4) with $A(c) = 0.07$ (0.10) $\mu\Omega$ cm K$^{-3/2}$. $\rho_{I\sigma}(T)$ for the specimen D, as seen from figure 10, vary nearly linearly with temperature down to 10 K with coefficients of 0.48 (0.62) $\mu\Omega$ cm K^{-1}. Tables 1 and 2 summarize the relevant physical parameters for these specimens.

4. Discussion

The temperature dependent part of the resistivity due to interface scattering is solely representative of its dynamic behaviour concerned with magnetic or spin scattering by magnetic impurities dissolved in the interface zone. For the specimen A, we observed at $T_{max} \approx 12$ K a resistivity maximum in the spin dependent interface resistivity, $\rho_{I\sigma}(T)$, and below it, $\rho_{I\sigma}(T)$ decreasing linearly in T to the residual resistivity at absolute zero. The resistivity maximum is the result of competition between the Kondo divergence on the single impurity and the 'freezing out' of the spin-flip scattering part of this resistivity. The temperature T_{max} can be considered as the strongly interacting spin temperature below which nearly all spins are strongly interacting. Physically, the level population of effective spins is diminishing at temperatures near T_f but starts to increase just above T_f. Correspondingly, the resistivity for the interacting spins, i.e., the first term on the right hand of (5), begins to slow in its rate of increase with temperature and ultimately at T_{max} it reaches a maximum and then decreases with further increasing temperature. Thus, T_{max} is expected to be close to T_f, and that is supported by the experimental results of T_f in Cu–(Ni, Fe) alloying systems that show $T_f = 12$–16 K depending on their compositions [36]. Of course, if there exists a progressive process of freezing-out of inelastic spin-flip scatterings, T_f may differs from T_{max}. On the other hand, the parameter T_m, which may contain the essential ingredients on which the effective free spin population depends, is found to be twice the resistivity maximum temperature in this model-fit scheme. However, no any physical idea can be gained through detailed studies because the relevant data from other magnetic measurements are unavailable at present.

One remarkable result of this model fit is the coefficient $A(c)$ that is roughly inversely proportional to the magnetic impurity concentration, i.e., $A(c) \sim 1/c$ [26]. It decreases comparatively from 0.11 (0.18) $\mu\Omega$ cm K$^{-3/2}$ for the specimens A to 0.07 (0.10) $\mu\Omega$ cm K$^{-3/2}$ for the specimen C. We take this to mean that the magnetic impurity concentration increases within the interface regions as a result of increasing interfacial disorder for the latter. However, for the specimens C, there is no maximum in $\rho_{I\sigma}(T)$ but a larger span of the $T^{3/2}$ behaviour as shown in figure 9. This can be qualitatively

understood as an indicator that the interaction between the magnetic impurities is strong enough to suppress the spin-flip scattering that is responsible for the Kondo resistivity, resulting in the absence of a maximum in the resistivity.

As illustrated in section 3, the $T^{3/2}$ behaviour is very sensitive to the availability of very long wavelength diffusion modes, i.e., those with a very small wave number q. If these modes are no longer operative, a T^2 dependence can supplant the $T^{3/2}$ behaviour at the lowest temperature. This accounts for the T^2 dependence observed for $\rho_{I\sigma}(T)$ for the specimen B (figure 8). Note that, in the quench condensed specimens, a large number of lattice defects is believed to be additionally introduced during the preparing process. Upon the progressively lowered defect concentration, the T^2 region will be less pronounced. In addition, our results show that the T^2 region extends with a shift of its interval to higher temperatures, indicating increasing impurity concentration at the interface zone.

In general, the initial $T^{3/2}$ dependence will gradually deviate towards an approximately linear dependence at higher temperatures or around the freezing temperature, and towards slower temperature variations at still higher temperatures. Thus, we believe that the linear T region of $\rho_{I\sigma}(T)$ for the specimen D (see figure 10) represents a slow transition between the T^2 and T_{max} regions. At low temperatures, the linear T dependence of the resistivity in dilute magnetic alloys has been predicted theoretically and is attributed to the short range interaction between magnetic impurities within the framework of a molecular field theory [39]; however, it has been known that this treatment is precluded from explaining the powers law in T of higher order in the low temperature resistivity. As a more adequate explanation, the present statement is supported by the experimental observation that there is a striking inflection-like feature of the interface resistivity curves around 10 K. This feature in $\rho_{I\sigma}(T)$ underlies a transition between the linear T and low temperature spin glass characteristic T^2 regions. Moreover, for this specimen with still increasing magnetic impurity concentration, a shift of T_{max} to higher temperature would be the most likely reason for observing such an extension of the linear T region in figure 10.

It should be pointed out in passing that, while much of the spin dependent interfacial resistivity is satisfactorily explained in terms of the concepts of local spin fluctuations and spin glass excitations, rigorous justification for Kondo effect and spin glass phenomena is still difficult to be made. This is partly because of insufficient information about magnetic impurity compositions, distribution and interactions between magnetic impurities in the interface regions, and partly because of the lack of experimental methods that give rise to direct evidence for these phenomena. Even so, it is physically meaningful to give the order of magnitude of the characteristic time of the spin fluctuation, τ_{sf}, and the relaxation time of the electrons. Since the Kondo temperature obtained from the spin-fluctuation theory is given by $kT_K^{sf} = \tau_{sf}^{-1}$ [31], the evaluation of τ_{sf} can be readily made by applying this relation between T_K and τ_{sf}. On the other hand, the relaxation time of the electrons can be described as τ_{v_F} $(= l/v_F)$. For the representative specimen A, we obtain $\tau_{sf}/\tau_{v_F} \sim 10^3$–$10^5$, provided that $T_K \approx$ 1–5 K, $l \sim$ 10–100 Å and $v_F \sim 10^8$ cm s^{-1}. This is in good agreement with the value of $T_F/T_K^{sf} \sim 10^4$, an alternative expression of the same ratio, where T_F represents the Fermi temperature. Fundamental to this study is that detection of a magnetic moment depends on the coherence time of the probe being used in relation to the characteristic spin fluctuation time τ_{sf} since the concepts of local spin fluctuations and spin glass excitations was invoked to account for our experimental data. The results that $\tau_{sf} \gg \tau_{v_F}$ show that isolated impurity atoms appear to be magnetic in the resistance study, suggesting a reasonable physical ground for our analysis of the experimental data. What is more, the applicability of Rivier's theory [26] to the situations in the specimens B, C and D means that the value of τ_{sf} is very large but finite, namely, the existence of a spin is taken for granted.

Apart from the above discussion of the low temperature resistivity data, we now intend to examine some relevant physical quantities in tables 1 and 2, such as the spin dependent resistivity data extrapolated at absolute zero as well as the spin asymmetry factors of α and μ. The factor μ was obtained from the above model fit; and α was calculated from the extrapolated values of the magnetoresistance at $T = 0$ K, using the relation of $\mathrm{MR} = [(\alpha - 1)/(\alpha + 1)]^2$. All these specimens under consideration indicate substantial residual values for the resistivities $\rho_F(0)$, $\rho_{AF}(0)$ and $\rho_{I\sigma}(0)$. As we might expect, the possible sources responsible for the resistivity behaviour are multiple; and they would be as follows: resonant scattering by magnetic (spin split) virtual bound states of 3d impurities, nonmagnetic type scattering by imperfections such as defects and the size effect on scattering of the conduction electrons. Note here that, though they include both elastic and inelastic scattering processes, the resistivity data cannot distinguish between them. The appearance of the substantial residual resistivity should be explained by resonant scattering by magnetic (spin split) virtual bound states of 3d impurities, especially by that occurring in the interface zone. This is supported by the finding of the same trend in the variation of the resistivities $\rho_F(0)$, $\rho_{AF}(0)$ and $\rho_{I\sigma}(0)$ from specimen to specimen, as viewed in tables 1 and 2. Of course, this does not mean that such a simple explanation gives rise to the whole story for the behaviour of the resistivity we observed. A complete understanding of this problem should be obtained by considering the interplay of all the possible sources mentioned above. For example, the extremely large values of the resistivity for the specimen A as compared to those of the other three are subject to the size effect on scattering of the conduction electrons. In addition, for the specimens B, C and D, though they all structurally have the same nominal form, a scatter in the values of the resistivities from specimen to specimen is observed. The difference is believed to be attributed to nonmagnetic type scattering by lattice defects that were additionally introduced during the preparing process. Also we notice that the data in tables 1 and 2 show that a large magnetoresistance results whenever the degree of spin asymmetry increases. A striking difference between the spin asymmetry factors α and μ is found in their size and structural dependence: the value of α is constantly larger than that of μ, and there is a significant spacer layer thickness dependence in the former one but not in the latter one. The implication in these results is that the specified features of spin dependent scatterings due to static ($T = 0$ K) and temperature-induced dynamical scattering processes are quite different. Physically, dynamical processes are often related to scatterings by magnons, phonons, spin fluctuations and spin glass phenomena, while static processes are representative of those by magnetic impurities and imperfections such as interface roughness and lattice defects. Hence, these results indirectly justify use of the concept of spin fluctuations and spin glass phenomena to analyse our low temperature resistivity data. The presence of the larger values of α reflects the stronger spin dependent scattering processes the conduction electrons experience at the absolute zero. In this scattering regime, rough interfaces and magnetic impurities proved themselves to have great influences upon spin dependent scattering of the conduction electrons. However, they would be of trifling importance while accounting for the large reduction in the value of α as the spacer layer thickness increases. Instead, the variation of the spin asymmetry factor as viewed in table 2 should be interpreted as a result of the size effect on spin dependent scattering of the conduction electrons.

Finally, some remarks should be made of the relation between the magnetoresistance at $T = 0$ K and correlated interface roughness based on the relevant quantities for the specimens B, C and D as listed in tables 1 and 2. As we have shown, the two aspects of interface roughness, interface disorder and interdiffusion, contribute in a quite different manner to spin dependent interface scattering and then the magnetoresistance.

The analysis of the interface resistivity data and the corresponding results reveal that more correlated interface roughness and less interdiffusion of magnetic impurities at interfaces tend to enhance the magnetoresistance. The observation means that the magnetoresistance increases with increasing topographical interface disorder, but with the requirement of less interdiffusion at interfaces. A recent quantum mechanical approach based on the Anderson model is available of treating scattering of the conduction electrons by random exchange potentials of magnetic impurities distributed randomly at interfaces in CoNi/Cu superlattices [30]. The work indeed demonstrated that the magnetoresistance increases with interface randomness, and that, upon increasing the population of magnetic impurity Ni concentration at the Cu spacer layer side of an interface, the magnetoresistance is largely reduced because the electronic states density at the Fermi level of the magnetic impurity becomes less spin dependent. This is qualitatively in close agreement with the present experimental findings. On the lines of the argument, our results seem in favour of the point of view that decrease of the magnetoresistance with increasing magnetic impurity concentration might be associated with an excessive accumulation of Ni impurity atoms around the interfaces due to interdiffusion. Even so, further experimental studies on this point are much expected.

5. Conclusions

In studying the low temperature resistivity and magnetoresistance in sputtered polycrystalline NiFeCo/Cu superlattices, we explored the temperature dependence of the interface resistivity for four specimens, one with $t_{Cu} = 9$ Å, and other three with $t_{Cu} = 21$–22 Å that are characterized by different correlated interface roughness. At low temperatures, we found, respectively, a resistivity maximum, T^2, $T^{3/2}$ and T power laws in the interface resistivity, with an increase in magnetic impurity concentration at interfaces. We attributed the dynamic behaviour of the interface resistivity to the presence of spin fluctuations and/or spin glass phenomena. This systematically explains why at low temperatures there is a variety of the behaviour in the temperature dependence of the magnetoresistance from specimen to specimen. The study showed that the rapid relaxation time of the conduction electrons makes the resistivity a nearly ideal probe to detect the variation of magnetic impurity concentration at interfaces. In this sense, we ascertained the two paramount aspects of interface roughness: interdiffusion across the interfaces and correlated roughness due to topographical interface disorder. The results demonstrated that the magnetoresistance increases with increasing correlated interface roughness and decreasing magnetic impurity concentration at interfaces, and that a large value of magnetoresistance results whenever the spin asymmetry is large.

Acknowledgments

The authors would like to thank Professor U Mizutani for generous support, Dr T Biwa for skilful technical assistance in this experiment, and Dr H Itoh for stimulating discussions. It is also the first author's pleasure to thank Dr W Zhao for her inspiration in the preparation of this paper.

References

[1] Barthélémy A, Fert A, Baibich M N, Hadjoudj S, Petroff F, Etienne P, Cabanel R, Lequien S, Nguyen Van Dau F and Creuzet G 1990 *J. Appl. Phys.* **67** 5908

[2] Petroff F, Barthélémy A, Hamzic A, Fert A, Etienne P, Lequien S and Creuzet G 1991 *J. Magn. Magn. Mater.* **93** 95

[3] Mosca D H, Petroff F, Fert A, Schroeder P A, Pratt W P Jr, Laloee R, and Lequien S 1991 *J. Magn. Magn. Mater.* **94** L1
[4] Mattson J E, Brubaker M E, Sowers C H, Conover M, Qiu Z and Bader S D 1991 *Phys. Rev.* B **44** 9378
[5] Sato H, Kobayashi Y, Aoki Y, Shintaku K, Hosoito N and Shinjo T 1993 *J. Phys. Soc. Japan* **62** L3380
[6] Saito Y, Inomata K, Uji S, Terashima T and Aoki H 1994 *J. Phys. Soc. Japan* **63** L1263
[7] Gijs M A M, Lenczowski S K J, van de Veerdonk R J M, Giesbers J B, Johnson M T and aan de Stegge J B F 1994 *Phys. Rev.* B **50** 16 733
[8] Kubota H, Sato M and Miyazaki T 1995 *Phys. Rev.* B **52** 343
[9] Suzuki M and Taga Y 1995 *Phys. Rev.* B **52** 361
[10] Camley R E and Barnas J 1989 *Phys. Rev. Lett.* **63** 664
[11] Barnas J, Fuss A, Camley R E, Grünberg P and Zinn W 1990 *Phys. Rev.* B **42** 8110
[12] Zhang S and Levy P M 1991 *Phys. Rev.* B **43** 11 048
[13] Fert A and Campbell I A 1971 *J. Physique Coll.* **32** C1-46
Fert A and Campbell I A 1976 *J. Phys. F: Met. Phys.* **6** 849
[14] Duvail J L, Fert A and Pereira L G 1994 *J. Appl. Phys.* **75** 7070
[15] Parkin S S P 1992 *Appl. Phys. Lett.* **61** 1358
[16] Diao Z T, Meguro K, Tsunashima S and Jimbo M 1996 *Phys. Rev.* B **53** 8227
[17] Diao Z T, Goto S, Meguro K, Tsunashima S and Jimbo M 1997 *J. Appl. Phys.* **81** 2327
[18] Jimbo M, Kanda T, Goto T, Tsunashima S and Uchiyama S 1992 *Japan. J. Appl. Phys.* **31** L1348
[19] Dieny B, Speriosu V S and Metin S 1991 *Europhys. Lett.* **15** 227
[20] Parkin S S P, Marks R F, Farrow R F C, Harp G R, Lam Q H and Savoy R J 1992 *Phys. Rev.* B **46** 9262
Renard J P, Beauvillan P, Dupas C, Le Dang K, Veillet P, Vélu E, Marlière C and Renard D 1992 *J. Magn. Magn. Mater.* **115** L147
[21] Cullen J R and Hathaway K B 1993 *Phys. Rev.* B **47** 14 998
[22] Mayadas A F, Janak J F and Gangulee A 1974 *J. Appl. Phys.* **45** 2780
[23] Dieny B, Speriosu V S, Nozières J P, Gurney B A, Vedyayev A and Ryzhanova N 1993 *Magnetism and Structure in System of Reduced Dimension (NATO ASI Series B 309)* ed R F C Farrow *et al* (New York: Plenum) p 279
[24] Garcia P F and Suna A 1983 *J. Appl. Phys.* **54** 2000
[25] Fert A 1991 *Science and Technology of Nanostructured Magnetic Materials, (NATO ASI Series B 259)* ed G C Hadjipanajis and G A Prinz (New York: Plenum) p 221
[26] River N and Adkins K 1975 *J. Phys. F: Met. Phys.* **5** 1745
[27] Sheikh A W 1988 *J. Phys. F: Met. Phys.* **18** 2015
[28] Riess I and Ron A 1973 *Phys. Rev.* B **8** 3467
Riess I and Ron A 1973 *Phys. Rev.* B **9** 2418
[29] Williams G, Swallow G A and Loram J W 1975 *Phys. Rev.* B **11** 344
[30] Itoh H 1996 *PhD Thesis* Department of Applied Physics, Nagoya University
see also Itoh H, Inoue J and Maekawa S 1993 *Phys. Rev.* B **47** 5809
Itoh H, Inoue J and Maekawa S 1995 *Phys. Rev.* B **51** 342
[31] River N and Zuckermann M J 1968 *Phys. Rev. Lett.* **21** 904
[32] Cornut B, Perrier J P, Tissier B and Tournier R 1971 *J. Physiqe Coll.* **32** C1 176
[33] Tournier R and Blandin A 1970 *Phys. Rev. Lett.* **8** 397
[34] Tholence J L and Tournier R 1970 *Phys. Rev. Lett.* **25** 867
Star W M, Basters F B, Nap G M, de Vroede E and van Baarle C 1972a *Physica* **58** 585
[35] Bennett L H, Swartzzendruber L J and Watson R E 1969 *Phys. Rev. Lett.* **23** 1171
[36] Cherenkov V A 1984 *Phys. Met. Metall.* **3** 177
[37] Berger L and deVroomen A R 1965 *J. Appl. Phys.* **36** 2777
Schindler A I and LaRoy B C 1966 *J. Appl. Phys.* **37** 3610
[38] Fenton E W 1973 *Phys. Rev.* **7** 3144
[39] Harrison R J and Klein M W 1967 *Phys. Rev.* B **154** 540